

# Novel Organic–Inorganic Hybrid Electrolyte to Enable LiFePO<sub>4</sub> Quasi-Solid-State Li-Ion Batteries Performed Highly around Room Temperature

Rui Tan,<sup>†,‡</sup> Rongtan Gao,<sup>†,‡</sup> Yan Zhao,<sup>†</sup> Mingjian Zhang,<sup>†</sup> Junyi Xu,<sup>§</sup> Jinlong Yang,<sup>\*,†</sup> and Feng Pan<sup>\*,†</sup>

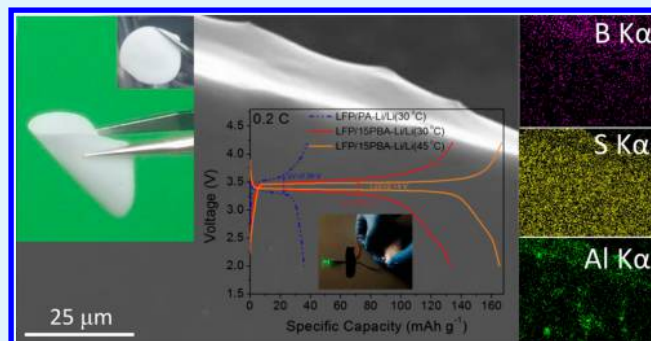
<sup>†</sup>School of Advanced Materials and Shenzhen Graduate School, Peking University, Shenzhen 518055, People's Republic of China

<sup>§</sup>Yunnan Metallurgical Group, Chuang Neng Al-air Battery, Co., LTD, Kunming 650500, People's Republic of China

## Supporting Information

**ABSTRACT:** A novel type of organic–inorganic hybrid polymer electrolytes with high electrochemical performances around room temperature is formed by hybrid of nanofillers, Y-type oligomer, polyoxyethylene and Li-salt (PBA-Li), of which the  $T_g$  and  $T_m$  are significantly lowered by blended heterogeneous polyethers and embedded nanofillers with benefit of the dipole modification to achieve the high Li-ion migration due to more free-volume space. The quasi-solid-state Li-ion batteries based on the LiFePO<sub>4</sub>/15PBA-Li/Li-metal cells present remarkable reversible capacities (133 and 165 mAh g<sup>-1</sup> @0.2 C at 30 and 45 °C, respectively), good rate ability and stable cycle performance (141.9 mAh g<sup>-1</sup> @0.2 C at 30 °C after 150 cycles).

**KEYWORDS:** polymers, hybrid electrolyte membranes, quasi-solid-state lithium ion batteries, stable performances, room temperature

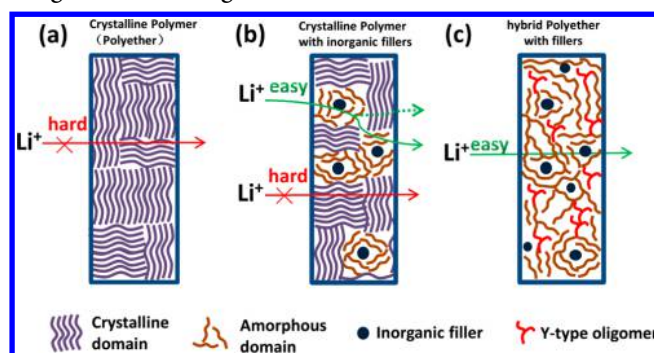


## INTRODUCTION

Organic liquid electrolytes play a crucial role in Li-ion batteries (LIBs), whereas they hinder the application range of LIBs because of the safety problem caused by flammable solvents.<sup>1</sup> Different from liquid electrolytes, solid polymer electrolytes (SPEs) applied for solvent-free all-solid-LIBs have captured more attention because of their potential advantages, including safety, wide electrochemical window, facile processability and low cost. It is observed that SPEs can hinder growth of lithium dendrites and make the application of lithium metal batteries possible.<sup>2,3</sup> Functioning as the separators in LIBs, the used polymers should maintain efficient Li-salt dissolvability, chemical and electrochemical stability with electrodes and fair flexibility.<sup>4–6</sup> For the sake of the above requirements, polyether based on oligoether ( $-\text{CH}_2-\text{CH}_2-\text{O}$ )<sub>n</sub> is widely utilized as one of the main parts of SPEs.<sup>3</sup>

Note that most polyethers are typical crystalline polymers at room temperature, Li-ions transfer hard due to low levels of segmental motions in the crystalline domains (described in Scheme 1a).<sup>7–9</sup> Such polyethers have to be used at a relatively high temperature. For example, poly(ethylene oxide) (PEO) mixed with Li-salt shows appropriate Li<sup>+</sup> conductivity (10<sup>-4</sup> S cm<sup>-1</sup>) only above 70 °C where the polymers reach its amorphous state.<sup>10</sup> According to our previous work, Li<sub>2</sub>FeSiO<sub>4</sub>/PEO/Li batteries were assembled and worked at 100 °C with a capacity of 258.2 mAh g<sup>-1</sup> at 1C. In this work, inorganic fillers were used to optimize the segmental mobility and ionic migration of polyether.<sup>11</sup> Meanwhile triboron-based

**Scheme 1. Basic Mechanisms of the Li-Ion Transfer Across (a) Crystalline Polymer, (b) Crystalline Polymer with Inorganic Fillers, and (c) Crystalline Polymer with Y-Type Oligomer and Inorganic Fillers**



(BPEG) electrolytes have also been investigated in Xu's group. With the assistance of PVDF, BPEG can be solidified to form quasi-solid membranes. Nevertheless, the BPEG/PVDF electrolytes need to work in LFP/Li cells at a relatively high temperature (>80 °C).<sup>12</sup> Single-ion triblock polymer (PS-PEO-PS) reported by M. Armand was used as SPEs in the LiFePO<sub>4</sub>/Li batteries operated at 60 °C.<sup>13</sup> Even addition of

Received: July 21, 2016

Accepted: October 27, 2016

Published: October 27, 2016

nanofillers and modification of polyether structures were used to optimize the SPEs performances respectively, the working temperature of such all-solid-state LIBs is still too high to fabricate commercial SPEs LIBs. Hence, decreasing the actual working temperature of SPEs is a crucial difficulty for the realization of the industrial production of SPEs-based LIBs.

Widening the operating temperature of SPEs can significantly extend the application range of SPEs-based LIBs. Closely related to the actual working temperature, the glass transition temperature ( $T_g$ ) and melting point ( $T_m$ ) are main pivotal factors which can reflect the levels of segmental mobility and crystalline to amorphous transition point. Lowering the  $T_g$  and  $T_m$  can effectively reduce the operating temperature of SPEs. Generally, three approaches have been carried out to change  $T_g$  and  $T_m$ : (i) addition of ceramic fillers to modify polyether dipole orientation and interrupt ordered structure, which gives a possibility of enhanced amorphicity further to facilitate Li-ion transfer (seen in Scheme 1b);<sup>14–17</sup> (ii) using branched or cross-linked polymers to change the structure of PEO;<sup>18–23</sup> (iii) addition of liquid components or large anion salts to the matrix of polyether to form a mixture.<sup>24–26</sup> With an empty p-orbitals and the  $sp^2$ -hybridized state, the boron atom serves as the cross-linking center to connect with linear oligomers then to form the oligomers with the planar structure. While combined with the crystalline polyether, BPEG with the remold and planar molecular structure can efficiently halt the order arrangement of linear chains, and indirectly enhance the ability of segmental motions, and further promote Li-migration. Utilizing boron-based molecular to form quasi-solid-state polymer membranes working around room temperature with success is reported in this work for the first time. In order to further improve the mechanical property of current SPEs, the hybrid membranes with optimized inorganic fillers and PEO can play a vital role. Optimization of organic molecules and addition of fillers can be simultaneously utilized to form a novel type of quasi-solid-state hybrid electrolytes, which are supposed to have excellent  $Li^+$  conductivity, good electrochemical stability, fair mechanical property, and the most important one, a low working temperature.

Herein, we reported a new type of organic–inorganic hybrid electrolyte membrane, which is comprised with nanosized  $Al_2O_3$  particles (30–50 nm), Y-type oligomer (BPEG), PEO and Li-salt (LiTFSI) (PEO/BPEG/ $Al_2O_3$ /LiTFSI, abbreviated as PBA-Li). As shown in Scheme 1c, due to the coworking optimization of fillers and blended polyethers, optimized PBA-Li membranes have lower  $T_g$  (–57.2 °C) and melting point (41.6 °C) and a higher  $Li^+$  conductivity ( $1.16 \times 10^{-2}$  mS  $cm^{-1}$  at 30 °C,  $7.71 \times 10^{-2}$  mS  $cm^{-1}$  at 45 °C) than the traditional PEO/ $Al_2O_3$ /LiTFSI-membranes (abbreviated as PA-Li) do. Notably, LiFePO<sub>4</sub>/15PBA-Li/Li batteries can be operated smoothly at 30 and 45 °C with high capacities (132.9 mAh  $g^{-1}$  and 165.1 mAh  $g^{-1}$  at 0.2 C) and good rate performance, as well as the remarkable cycling stability. This work supplies a way to prepare organic–inorganic hybrid membranes which will probably be used in commercial LIBs approaching room temperature in the future.

## EXPERIMENTAL SECTION

**Synthesis of Y-type BPEG.** The Y-type oligomer (BPEG) was synthesized by the reaction of poly(ethylene glycol) (PEG,  $M_w = 570$ –630) and borane ( $BH_3$ ). First of all, 5.4 g of PEG was dissolved in 20 mL of acetonitrile under nitrogen atmosphere and then the mixtures were stirred at 45 °C for half an hour. After that, 6 mL of borane

tetrahydrofuran complex solution (containing 6 mmol Borane, using excess  $BH_3$  assures all the raw PEG can be reacted.) was added at the rate of drop per five seconds by a constant pressure dropping funnel. The reaction was held under reflux for 24 h. After the reaction procedure, the acetonitrile and  $BH_3$  were removed by a rotary evaporator at 70 °C. Since the BPEG is sensitive to water, the product was then transferred into an Ar-filled glovebox and stored.

**Preparation of PBA-Li and PA-Li Membrane.** The obtained BPEG and the bis (trifluoromethane) sulfonimide lithium salt (LiTFSI) were dissolved in acetonitrile, with a molar ratio of ethylene oxide unit and lithium of 15:1. Then different ratio (5 wt %, 10 wt %, 15 wt %, 20 wt %, 50 wt %, 75 wt %) of poly(ethylene oxide) (PEO,  $M_w = 4 \times 10^6$ ) and 5 wt % of nanosize aluminum oxide ( $Al_2O_3$ , Sigma-Aldrich, the size is 30–50 nm) and were added into the above solution. The mixture was stirred for 24 h to form a homogeneous colloid. After that, cast the above mixture onto a Teflon substrate and heat it at 80 °C for 12 h to let the solvent evaporate and form a transparent membrane. Herein we obtained the PEO/BPEG/ $Al_2O_3$ /LiTFSI (PBA-Li) membrane. For comparison, we prepared the BPEG-free (PEO/ $Al_2O_3$ /LiTFSI, PA-Li) membranes, following the above steps without adding BPEG.

**Preparation of the Quasi-Solid-State LFP/Hybrid Electrolytes/Li Batteries.** The lithium iron phosphate (LFP), carbon black (CB) and poly(vinylidene fluoride) (PVDF), with a weight ratio of 5:3:2, were mixed up and grinded in NMP. Then cast the above mixture onto aluminum foil and heat it at 80 °C to obtain the cathode plate. The active materials (LFP) weight of every cathode electrode ranges from 0.7 to 1.0 mg and the area of those is 0.785  $cm^2$  (the diameter is 1 cm). Thus, the loading of LFP in every electrode ranges from 0.89 to 1.27  $mg\ cm^{-2}$ . Stack up LFP plate, the organic–inorganic hybrid electrolyte membranes (PBA-Li membrane, and PA-Li membrane for comparison) and Li plate seriatim to assemble the battery. Then the battery was sealed into a 2032 coin cell.

**Materials Characterization.** The X-ray diffraction (XRD) patterns of PBA-Li membrane,  $Al_2O_3$  and PEO were collected from a Bruker D8 Advance diffractometer using Cu– $K\alpha$  radiation at room temperature, from 10° to 80° (The scan speed is 1.15°  $min^{-1}$ ). The morphological characterization of PBA-Li membrane were observed by a scanning electron microscope (SEM, ZEISS Supra 55) while the composition and distribution of chemical elements were analyzed by energy X-ray spectroscopy (EDX, Oxford X-Max 20, 20 kV). The thermal stability of electrolyte membranes was studied by thermogravimetric analysis (TG) carried out on a TGA/DSC1 system. The glass transition temperature ( $T_g$ ) and melt temperature ( $T_m$ ) were studied by DSC (DSC1). The characteristic vibration of BPEG, PEG, PEO, PBA-Li membrane and PA-Li membrane were studied by FTIR (Frontier). The identification of H atom were studied by <sup>1</sup>H NMR (Advance 300, Bruker).

**Electrochemical Measurements.** The decomposition voltage were studied by electrochemical workstation (CHI 660E) between 0 and 6.0 V at a scan rate of 1 mV/s. The cyclic voltammetry (CV) results were conducted by electrochemical workstation (CHI 660E) between 2 and 4.2 V at a scan rate of 1 mV/s. The EIS spectra were obtained from 10 kHz to 0.1 Hz. Ionic conductivity and Electrochemical Impedance were studied by electrochemical workstation (PARSTAT 2273). The cells' electrochemical characteristics and polarization tests were performed on a Land instrument (Wuhan Land electronic Co., Ltd. China) with tests using cutoff voltages of 2 V (discharge) and 4.2 V (charge).

## RESULTS AND DISCUSSION

The Y-type oligomer (BPEG) can be synthesized through a facile method without any catalyst based on Xu's former work.<sup>12</sup> PEG and  $BH_3$ /THF are mixed in the  $CH_3CN$  solvent. After that, the mixture were stirring at 45 °C for 24 h. Then the products were obtained by removing the solvents and some part of unreacted ingredients. (Scheme 2) The FTIR spectra and NMR images are provided in Figure 1a and Figure S1 to characterize BPEG. In Figure 1a, apart from C–O–C (1110,

## Scheme 2. Chemical Reaction for the Synthesis of Y-Type Oligomer

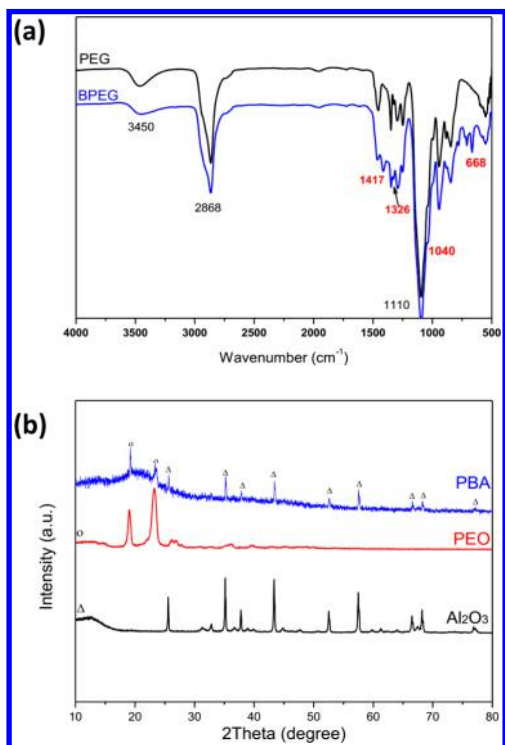
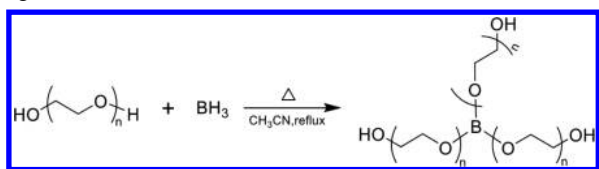


**Figure 1.** (a) FTIR spectra of PEG and as-synthesized BPEG from 4000 to 400  $\text{cm}^{-1}$  and (b) the XRD patterns of PBA, PEO and  $\text{Al}_2\text{O}_3$ , from  $10^\circ$  to  $80^\circ$ .

1200–1500  $\text{cm}^{-1}$ ) and  $\text{CH}_2$  (2868  $\text{cm}^{-1}$ ) vibration peak belonging to both BPEG and PEG, the bending stretch (668

$\text{cm}^{-1}$ ) and antisymmetric stretching (1326, 1417  $\text{cm}^{-1}$ ) vibration of B–O can be found in the FTIR curve of BPEG. In order to further analyze the structure of PEG and BPEG, the  $^1\text{H}$  NMR was carried out. Differing from PEG, the species of H increased, which can be identified on the chains of borate ester. FTIR and NMR results show that PEG chains can be linked to boron atom to form multibranch polymers. Such polymers are supposed to be added in the matrix of linear polyether to enhance the amorphicity then to facilitate Li-ion migration. For preparing PBA-Li membrane, nanosized  $\text{Al}_2\text{O}_3$  particles, Y-type oligomer (BPEG), PEO, and Li-salt (LiTFSI) are mixed in  $\text{CH}_3\text{CN}$  to form a homogeneous slurry at a certain proportion. Powder X-ray diffraction patterns for PBA-Li, PEO and  $\text{Al}_2\text{O}_3$  were shown in Figure 1b. The peaks in the patterns of PEO and  $\text{Al}_2\text{O}_3$  are obvious and sharp indicating the high degree of crystallinity, which can also be found in the corresponding peaks of the PBA pattern.

SEM and EDX were carried out to observe the morphologies and element distribution of PBA-Li membranes. The PBA-Li involved in SEM/EDS images consists of 15 wt % PEO, 5 wt % nanosized  $\text{Al}_2\text{O}_3$  and 80 wt % BPEG/LiTFSI (EO:Li = 15:1). As shown in Figure 2, the surface of PBA-Li membrane is smooth and no aggregate can be observed. The photos of PBA-Li membranes were shown, presenting that such polymer membranes are flexible. What's more, EDX mapping display the S, B, Al, C, O element distributions. The distribution of Al ( $\text{Al}_2\text{O}_3$ ), B (BPEG) and S (LiTFSI) elements are uniform through EDX mapping images, which further testifies the composites are homogeneous. Further to verify that BPEG can be solidified with PEO and nanosized  $\text{Al}_2\text{O}_3$  to form organic–inorganic hybrid electrolytes, the form of the raw BPEG, untreated hybrid electrolytes involving BPEG/PEG/nanosized  $\text{Al}_2\text{O}_3$  and prepared hybrid electrolytes are presented in the Figure S2. Notably, these membranes can be towed without any breakage directly demonstrating such membranes are quasi-solid state.

For analyzing the effects of different proportions of  $\text{Al}_2\text{O}_3$ , BPEG, and PEO on glass-state transition and amorphous transition, differential scanning calorimetry (DSC) was carried out. Figure 3a presents the changes of  $T_g$  and  $T_m$  in different samples.

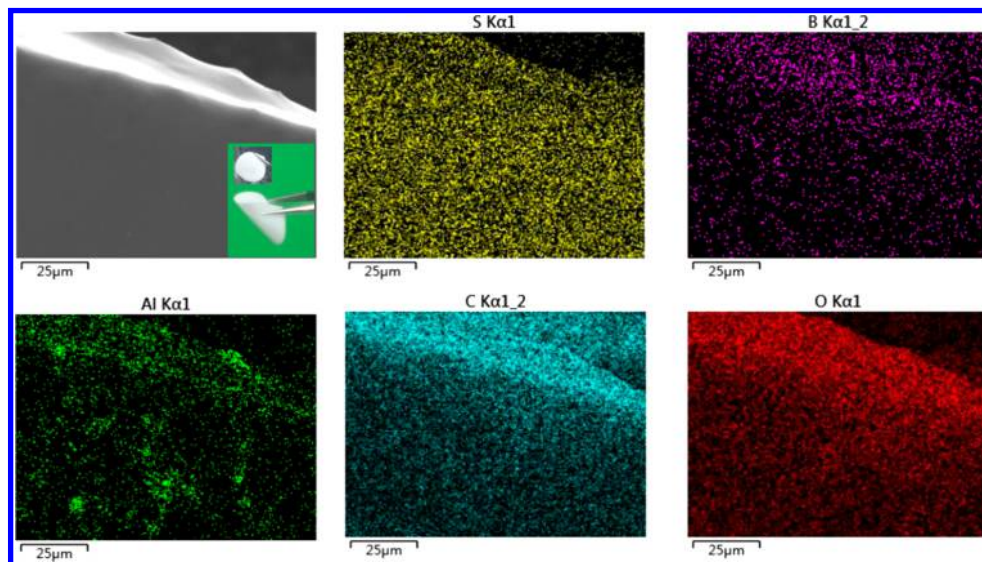


**Figure 2.** SEM images and EDX spectra for the surface of PBA-Li (the inset is the photo of 15PBA-Li membrane).

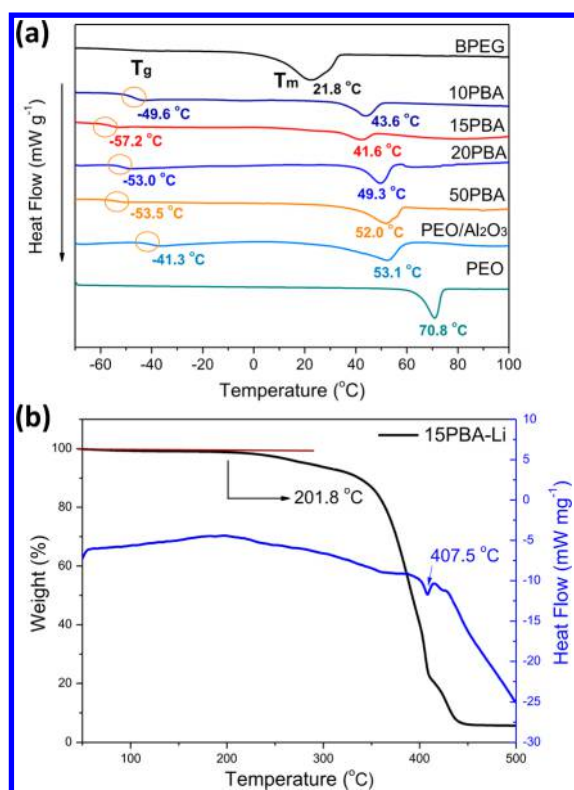


**Figure 3.** (a) DSC curves of different kinds of electrolyte membranes from  $-75$  to  $100$  °C and (b) the TGA-DSC curves for 15PBA-Li from  $30$  to  $500$  °C.

$T_g$  of raw PEO is not distinct but  $T_m$  is high up to  $70.8$  °C. It means that the improved level of amorphicity is poor when approaching to room temperature indicating the limited ability of segmental motion. With the addition of inorganic fillers ( $\text{Al}_2\text{O}_3$ ), an obvious reduction of  $T_g$  ( $-41.3$  °C) and  $T_m$  ( $53.1$  °C) was observed, which reveals the improved level of amorphicity due to the changed polyether dipole orientation as described in Scheme 1b. For further boosting the segment mobility and optimizing Li-ion transfer through electrolytes, the polyether (inorganic fillers included) were mingled with heterogeneous Y-type oligomer (BPEG). With the increase of Y-type polyether, the  $T_g$  and  $T_m$  get lower. 15PEO/B-PEG/ $\text{Al}_2\text{O}_3$  (meaning that the weight ratio of PEO in hybrid electrolytes is 15 wt %) membrane have the lowest  $T_g$  ( $-57.2$  °C) and  $T_m$  ( $41.6$  °C). Both utilizing fillers and introducing BPEG to the matrix of linear polyether can create more free volume with high segmental mobility in which Li ions are able to cross through organic-inorganic hybrid electrolytes favorably (as depicted by Scheme 1c). Based on the above analysis, the optimized membrane (15PEO/B-PEG/ $\text{Al}_2\text{O}_3$ , abbreviated as 15PBA-Li) was selected as the main object of study. In addition, the thermal stability of 15PBA-Li membrane was investigated by TGA-DSC. 15PBA-Li membranes were decomposed sharply from  $201.8$  to  $450$  °C in Figure 3b, indicating they are thermally stable below  $201.8$  °C. Thus, 15PBA-Li with good segmental mobility and high thermal stability might be beneficial for manufacture of safety quasi-solid-state LIBs.

After that, the electrochemical properties of 15PBA-Li membranes were further studied. Related to the intrinsic segmental mobility of polymers, impedance behaviors directly determine the performances of 15PBA-Li. Figure 4a presents

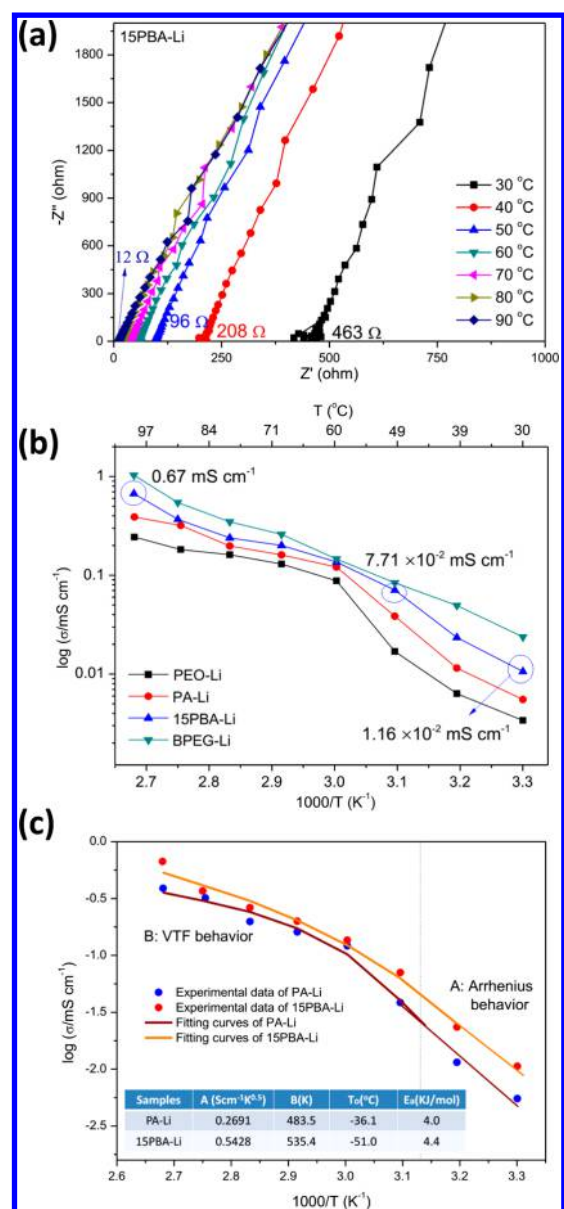


**Figure 4.** (a) EIS plots for 15PBA-Li at different temperatures, (b) Arrhenius plots of the ionic conductivity with varied temperatures for 15PBA-Li, PA-Li, PEO-Li, and BPEG-Li, and (c) fitting curves in orange and brown for the ionic conductivity experiment data of 15PBA-Li and PA-Li, inset is the basic factors obtained from the fitting curves based on the VTF equation.

the impedance behaviors of 15PBA-Li at various temperatures. From  $30$  to  $40$  °C, the values of impedance change from  $463$  to  $208$  Ω, and it further decreases to  $62$  and  $12$  Ω when heating to  $60$  and  $90$  °C, respectively. This also proves that the segmental motion improves and Li-ions migrate smoothly when 15PBA-Li gets amorphous states corresponding to the analyses of DSC data. Electrochemical impedance spectroscopy (EIS) was also performed to investigate the Li-ions kinetic properties. The ionic conductivity of different electrolytes can be obtained by the eq 1<sup>11,27</sup>

$$\sigma = L/(R \times S) \quad (1)$$

where  $L$  is the thickness of the electrolyte films,  $R$  is the resistance tested by EIS, and  $S$  is the area of the electrolyte films. Compared with PEO/LiTFSI, PA-Li membranes own

preferable Li-ion migration ability, ascribed to the polyether dipole modification by nanofillers and enhanced segmental motion. What's more, with the introduction of BPEG into the PA-Li membrane, 15PBA-Li membranes have much free volume with higher segmental mobility, in which Li-ions are able to cross through electrolytes favorably, showing higher ionic conductivity at multitemperatures. At room temperature, the ionic conductivity of 15PBA-Li is  $1.16 \times 10^{-2} \text{ mS cm}^{-1}$ , which is about 4 times that ( $3.0 \times 10^{-3} \text{ mS cm}^{-1}$ ) of PA-Li. (Figure 4b) BPEG/LiTFSI have the best Li-ion migration ability, but the poor mechanical property limits its application in hybrid electrolytes. As a result, 15PBA-Li membranes with decent ionic conductivity can be a good candidate as separators in LIBs. Further to investigate the mechanism of Li-ions migration, specific models should be discussed here, which can be generally divided into three items: Arrhenius model, Vogel–Tammann–Fulcher (VTF) model and the combination of them.<sup>28,29</sup> In details, Arrhenius model reveals that Li-ions can hop in the organic–inorganic hybrid electrolytes decoupled with the motion of the segmental. On the contrary, Li-ions can migrate along with the polymer branches or solvent molecular reflected by VTF model.<sup>30</sup> Herein, by fitting the prime experimental data, it is obvious that at low temperature (30–45 °C), the ionic conductivity  $\log\sigma$  shows an approximately linear relation with  $1/T$ , but there is nonlinear relation at comparatively high temperature (45–100 °C) seen in Figure 4c. Two different models are needed to explain these inconsecutive curves, in which the linear part (A in Figure 4c) and nonlinear part (B in Figure 4c) are corresponding to the Arrhenius eq 2<sup>31</sup> and VTF eq 3,<sup>32</sup> respectively

$$\sigma = A \times \exp\left(\frac{E_a}{RT}\right) \quad (2)$$

where the  $A$  is the pre-exponential factor and  $E_a$  is the activation energy for conductivity.

$$\sigma = AT^{-0.5} \times \exp\left[-\frac{B}{k(T - T_0)}\right] \quad (3)$$

where the  $A$  is the pre-exponential factor and  $B$  is the factor related to the activation energy for conductivity. Importantly,  $T_0$  is the key index at which the free volume to transfer Li-ions is zero. In other words, the value of  $(T - T_0)$  can reflect the quantities of free volume and the level of polymer segments' motion.<sup>33,34</sup> On the basis of the VTF equation, the factors  $A$ ,  $B$ ,  $T_0$ , and  $E_a$  can be obtained shown in the table of Figure 4c. Obviously, the  $T_0$  of 15PBA-Li is  $-51.0$  °C which is much lower than that ( $-36.1$  °C) of PA-Li, signifying that at the same  $T$ , 15PBA-Li owns much free volume with high motion of segments for Li-ions transferring. This analysis is consist of the explanation for changes of  $T_g$  and  $T_m$  in Figure 3a.

More importantly, the electrochemical stability is another key evaluation index for electrolytes. The linear sweep voltammetry (LSV) and polarization tests were carried out to study the real electrochemical windows of organic–inorganic hybrid electrolytes and the interface stability between electrolyte membranes and Li metals. From Figure 5a, the oxidation potential of 15PBA-Li is about 4.63 V, higher than the potential of PA-Li membranes (4.52 V), which is well matched with the voltage plateau for most of the cathode materials. For investigating the interface stability between electrolytes and Li metal, Li/hybrid electrolytes/Li cells were assembled and tested at 0.2 mA. At the initial cycle, the polarization potential of 15PBA-Li is 0.207

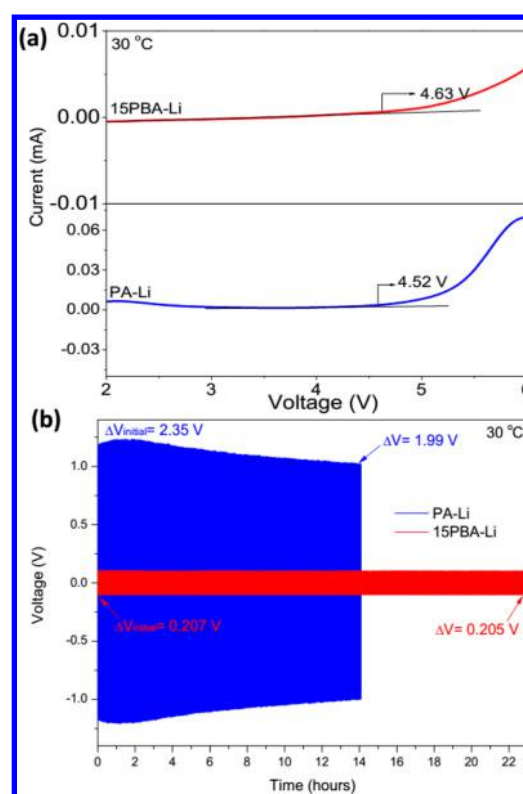


**Figure 5.** (a) Oxidation voltages of 15PBA-Li and PA-Li at 30 °C and (b) the polarization tests based on the charging–discharging current 0.2 mA for 15PBA-Li and PA-Li at 30 °C.

V lower than that (2.35 V) of PA-Li membrane with the same thickness, revealing the low internal resistance and superior Li-ion transfer ability of 15PBA-Li (in Figure 5b). During the repeated charging–discharging processes, the overpotential of Li/PA-Li/Li dramatically changes from 2.35 to 1.99 V just after 14 h, revealing unexpected side reactions occurs between the Li metal and PA-Li. On the contrary, the overpotential of Li/15PBA-Li/Li barely changes (from 0.207 to 0.205) after 23 h which means the compatibility between 15PBA-Li and Li metal is good. Furthermore, from long time polarization tests results shown in Figure S3, the Li dendrite can penetrate PA-Li membranes after polarization tests for approximately 78 h. However, it is noted that the 15PBA-Li can ensure Li metal working stably for 140 h without potential damages demonstrating PA-Li electrolytes possess good electrochemical stability and fair mechanical strength. Moreover, to investigate the mechanical strength of PA-Li membranes, Atomic Force Microscopy (AFM) at the Ar atmosphere was carried out to test the Young Modulus of PA-Li membranes (Figure S4). From Figure S4a, the mean modulus is 1.021 MPa and regional mean modulus with small amounts of  $\text{Al}_2\text{O}_3$  particles is still high up to 0.609 MPa. Additionally, the nanofillers can effectively promote the regional mechanical strength as shown in Figure S4b and c. This demonstrates PBA membranes have fair mechanical strength.

Quasi-solid-state LIBs were assembled with as-prepared 15PBA-Li membranes, Li metal anodes and commercial  $\text{LiFePO}_4$  (LFP) cathodes. For comparison, the PA-Li membranes were also utilized in Li/LFP batteries to test electrochemical performances as shown in Figure 6a to 6d. At 30 and 45 °C, the capacities of LFP/15PBA-Li/Li cells are 133.1 and 165.2  $\text{mAh g}^{-1}$  at 0.2 C, respectively, which are much

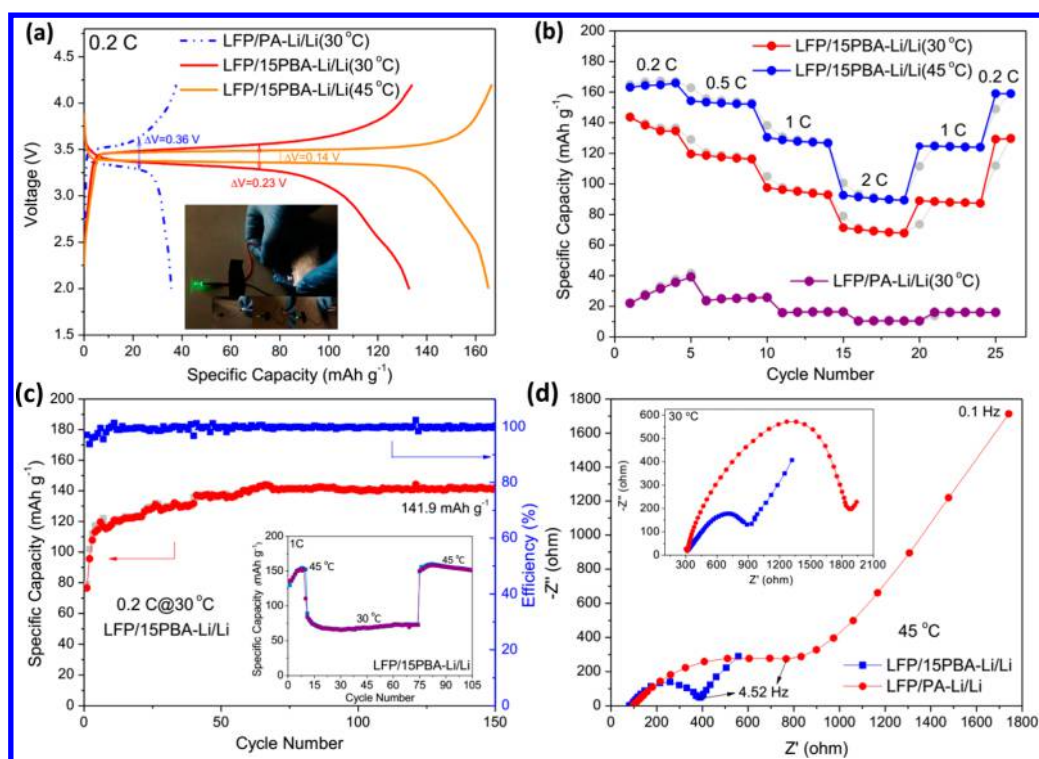


**Figure 6.** (a) Typical charge–discharge curves for LFP/15PBA-Li/Li cells and LFP/PA-Li/Li cells at 0.2 C. (Inset shows the LED light powered by large LFP/15PBA-Li/C batteries.) (b) Rate performances of LFP/15PBA-Li/Li cells and LFP/PA-Li/Li cells, (c) the cycling performances of LFP/15PBA-Li/Li at 0.2 C@30 °C (inset shows the cycling performances of LFP/15PBA-Li/Li cells from 45 to 30 °C then return to 45 °C at 1 C), and (d) the EIS plots for LFP/15PBA-Li/Li cells and LFP/PA-Li/Li cells at 30 °C (inset) and 45 °C.

higher than that ( $35.6 \text{ mAh g}^{-1}$  at 30 °C) of LFP/PA-Li/Li cells. Additionally, the overpotential ( $\Delta V$ ) of LFP/15PBA-Li/Li cells is lower than that of LFP/PA-Li/Li cells in Figure 5a, which is consistent with the CV results in Figure S5. Lower  $\Delta V$  reflects a lower internal resistance and a better Li-ion migration ability of PBA-Li membranes as separators owing to much free-volume space for segment motion. It is worth mentioning that 15PBA-Li membrane was also used in LFP/Carbon large batteries to power the LED lights at room temperature (inset of Figure 6a and S2e). Even this battery was folded and distorted, the LED was still glowing, which indicates the safety and flexibility of PBA-Li membranes.

LFP/15PBA-Li/Li cells exhibits the good rate capability and cycle performances at 30 and 45 °C shown in Figure 6b and c. The reversible capacity is high as 134.6, 117.8, 97.5, and  $71.2 \text{ mAh g}^{-1}$  at 0.2, 0.5, 1, and 2 C at 30 °C, which can be returned to  $130.2 \text{ mAh g}^{-1}$  at 0.2 C. At 45 °C, the preferable rate performances were obtained with 164.7, 153.6, 130.2, and  $93.5 \text{ mAh g}^{-1}$  at 0.2, 0.5, 1, and 2 C. However, the rate performances of LFP/PA-Li/Li cells is very poor whose capacity is below  $40 \text{ mAh g}^{-1}$  at various current rates. Compared with LFP/PA-Li/Li cells, such LFP/15PBA-Li/Li cells have much higher reversible capacity due to the good ionic conductivity and high segment mobility coming from the organic–inorganic coworking optimization, in which inorganic fillers can modify polyether dipole orientation and blended polyether is able to prevent oligoether-crystallinity. For cycling performances, at 30 °C, LFP/15PBA-Li/Li cells can operate favorably with  $141.9 \text{ mAh g}^{-1}$  at 0.2 C for 150 cycles, whereas the initial capacity of batteries with BPEG/PVDF membranes is low to  $10 \text{ mAh g}^{-1}$  at 0.3 C @25 °C in the former work, indirectly reflecting PVDF with infirm ability and limited space to accommodating Li-ions

migrating restricts the electrochemical properties and performances of PVDF/BPEG.<sup>12</sup> Inset of Figure 6c and S6 show that from 45 to 30 °C then back to 45 °C LFP/15PBA-Li/Li cells can work with reversible capacities of 154.0 to 72 then to  $155.9 \text{ mAh g}^{-1}$  at 1 C indicating such quasi-solid cells can fit different working temperature even at the room temperature. While at 30 °C, the reversible capacity of LFP/PA-Li/Li cells is just  $11.9 \text{ mAh g}^{-1}$  at 1 C. Specially the LFP/15PBA-Li/Li cells were tested at 5 C to investigate the high rate performance at room temperature. As depicted in Figure S7, at 30 °C, the initial capacity of LFP/15PBA-Li/Li cells is  $37.3 \text{ mAh g}^{-1}$  at 5 C. And after 150 cycles, the capacity increased to over  $46.0 \text{ mAh g}^{-1}$  and maintains steady. Different from LFP/PA-Li/Li cells, LFP/15PBA-Li/Li cells with high reversible capacity and superior rate ability can be a good selection for manufacture of quasi-solid-state batteries applying for electric vehicles.

For further clarifying reasons behind the good performances of LFP/15PBA-Li/Li cells at both 30 and 45 °C, electrochemical impedance spectroscopy (EIS) was performed. From Nyquist plots (Figures 6d and S8), semicircle and line regions are observed, in which the semicircle at the high frequency region is described to the charge transfer resistance ( $R_{ct}$ ) at the cathode/electrolyte interface and the line region at the low frequency region is ascribed to resistance ( $R_w$ ) of Li-ion migration. The  $R_{ct}$  value of LFP/15PBA-Li/Li cells at 30 °C is about  $658 \Omega$ , which is lower than that of LFP/PVDF/BPEG-Li/Li<sup>12</sup> (above  $8 \text{ k}\Omega$ , leading to hard Li-ion transformation at room temperature) and LFP/PA-Li/Li cells (above  $1 \text{ k}\Omega$ , inset of Figure 6d), which further demonstrates these hybrid electrolytes with low  $T_m$  and  $T_g$  possess more free space with high segmental mobility for Li-ions migrating due to the coworking optimization of fillers and blended polyether.

Coincidentally, comparing with LFP/PA-Li/Li cells, LFP/1SPBA-Li/Li cells own much lower resistance (291  $\Omega$ ) at 45 °C revealing the temperature-activated process can not only improve the segment motion of polymers but also promote the compatibility between polymers and electrodes. Apart from temperature-activated process, electrochemical pretreatments were also studied. From Figure S8, the  $R_{ct}$  of LFP/1SPBA-Li/Li cells changes from 870 to 540  $\Omega$  at 30 °C after electrochemical pretreatments, which can optimize the interface and allow Li-ions to transport with continuous hopping between sites of tunnels formed by organic–inorganic composites with high segmental mobility. Thus, with the organic–inorganic optimization, the 1SPBA-Li electrolytes ensure the quasi-solid batteries can operate favorably with good electrochemical performances with relatively low internal resistance.

## CONCLUSION

In summary, for widening the working temperature of polyether based electrolytes, a novel type of organic–inorganic hybrid electrolytes was prepared with nanosized  $Al_2O_3$  particles, Y-type polyether (BPEG), PEO and Li-salt (LiTFSI). of which the  $T_g$  and  $T_m$  are significantly lowered by blended heterogeneous polyethers and embedded nanofillers with benefit of the dipole modification to achieve the high Li-ion migration due to more free-volume space. LFP/1SPBA-Li/Li cells operate smoothly at 30 and 45 °C with remarkable reversible capacity (133.1, 165.2 mAh  $g^{-1}$  at 0.2C respectively) and better rate ability at 30 and 45 °C, as well as the more stable cycle performance than LFP/PA-Li/Li cells. Moreover this facile organic–inorganic hybrid electrolytes fabricating method makes 1SPBA-Li membranes to be an excellent candidate in the manufacture of advanced quasi-solid batteries.

## ASSOCIATED CONTENT

### Supporting Information

The Supporting Information is available free of charge on the ACS Publications website at DOI: 10.1021/acsami.6b09008.

Detailed description of the experiments and additional figures about FTIR/NMR characterization and electrochemical performance (PDF)

## AUTHOR INFORMATION

### Corresponding Authors

\*E-mail: yangjl@pkusz.edu.cn.

\*Tel: 86-755-26033200. E-mail: panfeng@pkusz.edu.cn.

### Author Contributions

<sup>‡</sup>R.T. and R.G. contributed equally to this work.

### Notes

The authors declare no competing financial interest.

## ACKNOWLEDGMENTS

The research was financially supported by National Materials Genome Project (2016YFB0700600), National Science Foundation of China (No. 51602009), Guangdong Innovation Team Project (No. 2013N080) and Shenzhen Science and Technology Research Grant (No. JCYJ20140903101633318, peacock plan KYPT20141016105435850).

## REFERENCES

(1) (a) Xu, K. Nonaqueous Liquid Electrolytes for Lithium-Based Rechargeable Batteries. *Chem. Rev.* **2004**, *104*, 4303–4417. (b) Zheng, J.; Liu, T.; Hu, Z.; Wei, Y.; Song, X.; Ren, Y.; Wang, W.; Rao, M.; Lin,

Y.; Chen, Z.; Lu, J.; Wang, C.; Amine, K.; Pan, F. Tuning of Thermal Stability in Layered Li ( $Ni_xMn_yCo_z$ ) $O_2$ . *J. Am. Chem. Soc.* **2016**, *138*, 13326–13334. (c) Wei, Y.; Zheng, J.; Cui, S.; Song, X.; Su, Y.; Amine, K.; Pan, F. Kinetics Tuning of Li-ion Diffusion in Layered Li( $Ni_xMn_yCo_z$ ) $O_2$ . *J. Am. Chem. Soc.* **2016**, *137*, 8364–8367.

(2) Oudenhoven, J. F. M.; Baggetto, L.; Notten, P. H. L. All-Solid-State Lithium-Ion Microbatteries: A Review of Various Three-Dimensional Concepts. *Adv. Energy Mater.* **2011**, *1*, 10–33.

(3) Xu, K. Electrolytes and Interphases in Li-Ion Batteries and Beyond. *Chem. Rev.* **2014**, *114*, 11503–11618.

(4) Li, J.; Lin, Y.; Yao, H.; Yuan, C.; Liu, J. Tuning Thin-Film Electrolyte for Lithium Battery by Grafting Cyclic Carbonate and Combed Poly(ethyleneoxide) on Polysiloxane. *ChemSusChem* **2014**, *7*, 1901–1908.

(5) Patel, M.; Bhattacharyya, J. A. A Crosslinked “Polymer–Gel” Rechargeable Lithium-Ion Battery Electrolyte from Free Radical Polymerization Using Nonionic Plastic Crystalline Electrolyte Medium. *Energy Environ. Sci.* **2011**, *4*, 429–432.

(6) Lee, S.-I.; Schömer, M.; Peng, H.; Page, K. A.; Wilms, D.; Frey, H.; Soles, C. L.; Yoon, D. Y. Correlations between Ion Conductivity and Polymer Dynamics in Hyperbranched Poly(ethylene oxide) Electrolytes for Lithium-Ion Batteries. *Chem. Mater.* **2011**, *23*, 2685–2688.

(7) Yang, L. Y.; Wei, D. X.; Xu, M.; Yao, Y. F.; Chen, Q. Transferring Lithium Ions in Nanochannels: A PEO/Li<sup>+</sup> Solid Polymer Electrolyte Design. *Angew. Chem., Int. Ed.* **2014**, *53*, 3631–3635.

(8) Ma, Q.; Zhang, H.; Zhou, C.; Zheng, L.; Cheng, P.; Nie, J.; Feng, W.; Hu, Y. S.; Li, H.; Huang, X.; Chen, L.; Armand, M.; Zhou, Z. Single Lithium-Ion Conducting Polymer Electrolytes Based on a Super Delocalized Polyanion. *Angew. Chem., Int. Ed.* **2016**, *55*, 2521–2525.

(9) Kaczmarek, H. Mechanism of Photoinitiated Degradation of Poly(ethylene oxide) by Copper Complexes in Acetonitrile. *J. Photochem. Photobiol., A* **1996**, *95*, 61–65.

(10) Appetecchi, G. B.; Zane, D.; Scrosati, B. PEO-Based Electrolyte Membranes Based on LiBC<sub>4</sub>O<sub>8</sub> Salt. *J. Electrochem. Soc.* **2004**, *151*, A1369–A1374.

(11) Tan, R.; Yang, J.; Zheng, J.; Wang, K.; Lin, L.; Ji, S.; Liu, J.; Pan, F. Fast Rechargeable All-Solid-State Lithium Ion Batteries with High Capacity Based on Nano-sized Li<sub>2</sub>FeSiO<sub>4</sub> Cathode by Tuning Temperature. *Nano Energy* **2015**, *16*, 112–121.

(12) Xu, J.; Li, J.; Zhu, Y.; Zhu, K.; Liu, Y.; Liu, J. A TriPEG-boron Based Electrolyte Membrane for Wide Temperature Lithium Ion Batteries. *RSC Adv.* **2016**, *6*, 20343–20348.

(13) Bouchet, R.; Maria, S.; Meziane, R.; Aboulaich, A.; Lienafa, L.; Bonnet, J. P.; Phan, T. N.; Bertin, T. D.; Gignes, D.; Devaux, D.; Denoyel, R.; Armand, M. Single-ion BAB Triblock Copolymers as Highly Efficient Electrolytes for Lithium-metal Batteries. *Nat. Mater.* **2013**, *12*, 452–457.

(14) Lago, N.; Garcia-Calvo, O.; Lopez del Amo, J. M.; Rojo, T.; Armand, M. All-Solid-State Lithium-Ion Batteries with Grafted Ceramic Nanoparticles Dispersed in Solid Polymer Electrolytes. *ChemSusChem* **2015**, *8*, 3039–3043.

(15) Manuel Stephan, A.; Nahm, K. S. Review on Composite Polymer Electrolytes for Lithium Batteries. *Polymer* **2006**, *47*, 5952–5964.

(16) Do, N. S. T.; Schaeztl, D. M.; Dey, B.; Seabaugh, A. C.; Fullerton-Shirey, S. K. Influence of Fe<sub>2</sub>O<sub>3</sub> Nanofiller Shape on the Conductivity and Thermal Properties of Solid Polymer Electrolytes: Nanorods versus Nanospheres. *J. Phys. Chem. C* **2012**, *116*, 21216–21223.

(17) Tominaga, Y.; Yamazaki, K. Fast Li-ion Conduction in Poly(ethylenecarbonate)-based Electrolytes and Composites Filled with TiO<sub>2</sub> nanoparticles. *Chem. Commun.* **2014**, *50*, 4448–4450.

(18) Münchow, V.; Di Noto, V.; Tondello, E. Poly[(oligoethylene glycol) dihydroxytitanate] as Organic-inorganic Polymer-electrolytes. *Electrochim. Acta* **2000**, *45*, 1211–1221.

(19) Aydın, H.; Şenel, M.; Erdem, H.; Baykal, A.; Tülü, M.; Ata, A.; Bozkurt, A. Inorganic–organic Polymer Electrolytes Based on

Poly(vinyl alcohol) and Borane/poly(ethylene glycol) Monomethyl Ether for Li-ion Batteries. *J. Power Sources* **2011**, *196*, 1425–1432.

(20) Shim, J.; Kim, D.-G.; Lee, J. H.; Baik, J. H.; Lee, J.-C. Synthesis and Properties of Organic/inorganic Hybrid Branched-graft Copolymers and Their Application to Solid-state Electrolytes for High Temperature Lithium-ion batteries. *Polym. Chem.* **2014**, *5*, 3432–3442.

(21) Niitani, T.; Shimada, M.; Kawamura, K.; Dokko, K.; Rho, Y.-H.; Kanamura, K. Synthesis of Li<sup>+</sup> Ion Conductive PEO-PSt Block Copolymer. Electrolyte with Microphase Separation Structure. *Electrochem. Solid-State Lett.* **2005**, *8*, A385–388.

(22) Zhang, H.; Kulkarni, S.; Wunder, S. L. Blends of POSS-PEO(*n* = 4)<sub>8</sub> and High Molecular Weight Poly(ethylene oxide) as Solid Polymer Electrolytes for Lithium Batteries. *J. Phys. Chem. B* **2007**, *111*, 3583–3590.

(23) Pennarun, P.-Y.; Jannasch, P. Electrolytes Based on LiClO<sub>4</sub> and Branched PEG-Boronate Ester Polymers for Electrochromics. *Solid State Ionics* **2005**, *176*, 1103–1112.

(24) Liang, B.; Tang, S.; Jiang, Q.; Chen, C.; Chen, X.; Li, S.; Yan, X. Preparation and Characterization of PEO-PMMA Polymer Composite Electrolytes Doped with Nano-Al<sub>2</sub>O<sub>3</sub>. *Electrochim. Acta* **2015**, *169*, 334–341.

(25) Xiao, Q.; Wang, X.; Li, W.; Li, Z.; Zhang, T.; Zhang, H. Macroporous Polymer Electrolytes Based on PVDF/PEO-*b*-PMMA Block Copolymer Blends for Rechargeable Lithium Ion Battery. *J. Membr. Sci.* **2009**, *334*, 117–122.

(26) Pandey, G. P.; Kumar, Y.; Hashmi, S. A. Ionic Liquid Incorporated PEO Based Polymer Electrolyte for Electrical Double Layer Capacitors: A Comparative Study with Lithium and Magnesium Systems. *Solid State Ionics* **2011**, *190*, 93–98.

(27) Lin, Y.; Li, J.; Liu, K.; Liu, Y.; Liu, J.; Wang, X. Unique Starch Polymer Electrolyte for High Capacity All-Solid-State Lithium Sulfur Battery. *Green Chem.* **2016**, *18*, 3796–3803.

(28) Agrawal, R. C.; Pandey, G. P. Solid Polymer Electrolytes: Materials Designing and All-solid-state Battery Applications: an Overview. *J. Phys. D: Appl. Phys.* **2008**, *41*, 223001–223019.

(29) Quartarone, E.; Mustarelli, P. Electrolytes for Solid-State Lithium Rechargeable Batteries: Recent Advances and Perspectives. *Chem. Soc. Rev.* **2011**, *40*, 2525–2540.

(30) Ratner, M. A.; Johansson, P.; Shriver, D. F. Polymer Electrolytes: Ionic Transport Mechanisms and Relaxation Coupling. *MRS Bull.* **2000**, *25*, 31–37.

(31) Li, Y.-H.; Wu, X.-L.; Kim, J.-H.; Xin, S.; Su, J.; Yan, Y.; Lee, J.-S.; Guo, Y.-G. A Novel Polymer Electrolyte with Improved High-Temperature-Tolerance up to 170 °C for High-Temperature Lithium-Ion Batteries. *J. Power Sources* **2013**, *244*, 234–239.

(32) Kumar, Y.; Pandey, G. P.; Hashmi, S. A. Gel Polymer Electrolyte Based Electrical Double Layer Capacitors: Comparative Study with Multiwalled Carbon Nanotubes and Activated Carbon Electrodes. *J. Phys. Chem. C* **2012**, *116*, 26118–26127.

(33) Cohen, M. H.; Turnbull, D. Molecular Transport in Liquids and Glasses. *J. Chem. Phys.* **1959**, *31*, 1164–1169.

(34) Gibbs, J. H.; DiMarzio, E. A. Nature of the Glass Transition and the Glassy State. *J. Chem. Phys.* **1958**, *28*, 373–383.